

CONCRETE LIBRARY OF JSCE NO. 11. JUNE 1988

ANALYSIS OF DAMAGES INFLICTED ON REINFORCED CONCRETE VIADUCTS
DURING THE MIYAGIKEN-OKI EARTHQUAKE

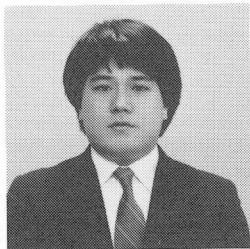
(Translation from Proceedings of JSCE, Vol.384/V-7, August 1987)



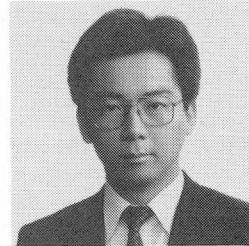
Yoshio OZAKA



Motoyuki SUZUKI



Yasushi TAKEYAMA



Harumi KIKUCHI

SYNOPSIS

In the Miyagiken-oki Earthquake (1978), mid-height beams in reinforced concrete (RC) viaducts of the Tohoku Shinkansen were subjected to considerable damage. The purpose of this study is to investigate analytically and statistically the causes of the varying degrees of damage in mid-height beams according to district or ground type. As a result, a close correlation is observed between the degree of damage in mid-height beams and the beam yielding seismic coefficient (base shear coefficient). Also, the necessity of reexamining the coefficients according to ground types in aseismic design is pointed out.

Yoshio OZAKA. BSc. MSc. PhD Engineering, Tohoku University, SENDAI. Senior Engineer, Structures Design Office, '66 and Deputy Director, Osaka Construction Bureau, '70, Japanese National Railways. Professor of Structural Engineering, Tohoku University, since '72. MEMBERSHIPS: Delegation of Japan to CEB; Commission "Seismic Design" of FIP; ACI; IABSE; JSCE; JCI; JPCEA. Japan Railway Eng. Ass. Meritorious Paper Award for study of PC through-girder bridge, '67; JSCE Award (Yoshida Prize) for study of quality control of field concrete, '68; JCI Award for study of cracking behavior of RC tension member under drying, '86.

Motoyuki SUZUKI is a research associate of the Department of Civil Engineering at Tohoku University, SENDAI, Japan. He received his Master of Engineering Degree in 1977 from Tohoku University. His research interests include behavior of reinforced concrete structure during earthquake, and reliability problems in reinforced concrete structure. He is a member of ACI, IABSE, JSCE, and JCI.

Yasushi TAKEYAMA is a research associate of the Department of Civil Engineering at Tohoku University, SENDAI, Japan. He received his Master of Engineering Degree in 1983 from Tohoku University. He is a member of JSCE.

Harumi KIKUCHI is a government official of National Land Agency, TOKYO, Japan. He received his Master of Engineering Degree in 1985 from Tohoku University.

1. INTRODUCTION

Severe and widespread damage due to flexural-shear occurred in the mid-height beams and columns of reinforced concrete viaducts of the Tohoku Bullet Train Line when it was under construction during the Miyagiken-oki earthquake (1978 June) [1]. The mid-height beams parallel to the track and perpendicular to the track were constructed with the intention of reducing the bending moment in columns of viaducts not less than 10 m in height. However, the mid-height cross beams perpendicular to the track were subjected to considerable damage due to alternating flexural-shear [2]. At the time there were 149 RC viaducts with 3 or 4 spans in Miyagi prefecture. Figure 1 shows the degree of damage to the viaducts. In this figure, the maximum crack width in the mid-height cross beams is considered to be the damage index. The reasons for adopting such an index are as follows: (1) the occurrence of cracks in other members appeared only where crack formation in mid-height cross beams also occurred, (2) the rates of crack occurrences in other members were in considerable correlation with those in mid-height beams, and (3) in the aftermath of the earthquake, when determining the repair method for damaged mid-height beams, the degree of the maximum crack width had already been taken into consideration.

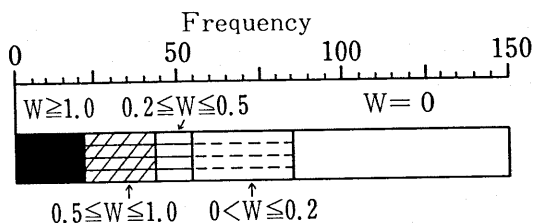
The RC viaducts of the Tohoku Bullet Line have almost the same structure in all districts and for all ground types, in spite of their different vibration characteristics. Therefore, it is significant that an established aseismic design method for RC structures suffered from varying degrees of damage in the Miyagiken-oki earthquake. In other words, data on the damages which occurred during this earthquake are thought to be valuable in considering vibration characteristics of members and structure or ground type for the purpose of practical aseismic design.

In consideration of the above view point, static and dynamic elasto-plastic analyses of viaducts were conducted on the basis of the load-displacement relationships of RC members obtained from our experiment. These analyses were done in order to determine the causes of damages to mid-height beams and the varying degrees of damage according to district or ground type. Also, the relationship between the damage index and structural conditions, ground conditions, foundation conditions, and so on, were examined statistically. Finally, we determined whether or not the existing aseismic design provides adequate protection against earthquake by means of probabilistic models of resistance of structure and applied earthquake force.

2. STATIC ELASTO-PLASTIC ANALYSIS OF RC VIADUCTS AND EARTHQUAKE DAMAGES

2.1 Modeling of RC Viaduct

Since the Tohoku Bullet Line runs north and south in the Tohoku district and the seismic focus of the Miyagiken-oki earthquake was located at about 110 km to the east of Miyagi prefecture, RC viaducts were assumed to have been hit with strong vibrations from the direction perpendicular to the track. This assumption was supported by the fact that earthquake damages were concentrated in mid-height cross beams. It was also observed that the degree of damages was greater in intermediate viaducts than in end viaducts [1]. The reason for this difference is as follows: the main reinforcement ratios of columns or beams in end viaducts were higher and therefore member resistance in end viaducts was greater than in intermediate viaducts. For the reasons mentioned above, the plane viaducts perpendicular to the track in intermediate blocks are the subject of this study (see Fig. 2).



W: Crack width in mid-height beam

Fig. 1 Damage rank of mid-height beam

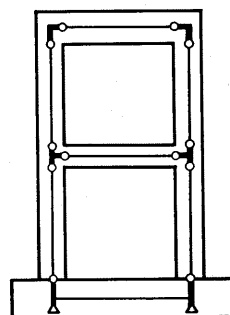


Fig. 2 Plane rigid frame

The following assumptions were considered in this analysis:

1. The displacement of each nodal point occurs in the plane, and torsion is not taken into consideration.
2. Each member is modeled by the straight line connecting the axial line of each member, and the portions intersecting axial lines are assumed to be rigid.
3. Stress and strain due to dead load are not taken into consideration.
4. Response in each load increment is linear.

2.2 Modeling of Member

It is necessary to use an appropriate model, indicating the stiffness of the member or the characteristics of the energy absorption of the member, in order to analyze the response of the RC structure during an earthquake. In this study, an end elasto-plastic spring model [3],[4] is used (see Fig. 3). The advantages of this model are as follows:

1. Experimental data of the member under alternating cyclic loading can be used.
2. Energy absorption of the member end (in the case of this model under loading with constant amplitude) is approximately equal to that in the case of the discrete spring model [5].

2.3 Modeling of Skelton Curve of Member

(1) Principle

A skelton curve of the member was modeled by means of three straight lines connecting the origin O, the occurrence of the flexural crack C, the point of member yield Y, and the point of ultimate U (see Fig. 4). The flexural crack was assumed to occur when concrete fiber stress of the tension zone reached concrete tensile strength. The load at yielding of the tension bar was assumed to be the load at the point of member yielding; in calculating the displacement at the point of member yielding, additional displacement due to elongation of tension bars was taken into consideration, in addition to displacement due to flexure. Furthermore, the load at the crush of concrete in the compression zone was assumed to be the load of the ultimate; in calculating the displacement at the ultimate, twice the additional displacement due to elongation of tension bars was taken into consideration, in addition to displacement due to flexure [6].

(2) Materials

The stress-strain curve of concrete by ACI [7] was used in this study (see Fig. 5(a)). The stress-strain curve of the bar was determined by a tension test (see Fig. 5(b)). In this analysis, $f_c' = 270\text{kgf/cm}^2$, $f_y = 3750\text{kgf/cm}^2$ and $f_u = 4500\text{kgf/cm}^2$.

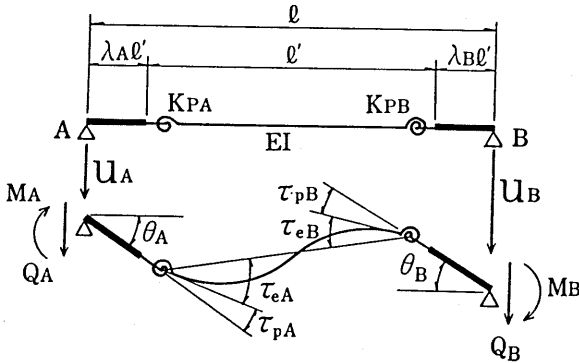


Fig. 3 End elasto-plastic spring model for member

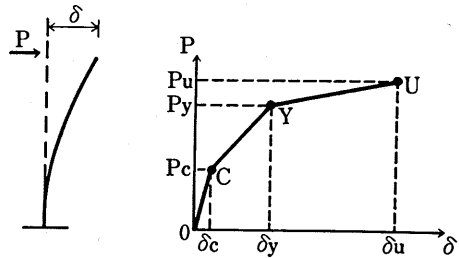
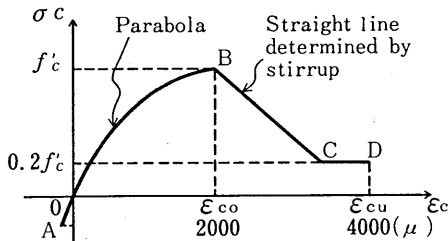
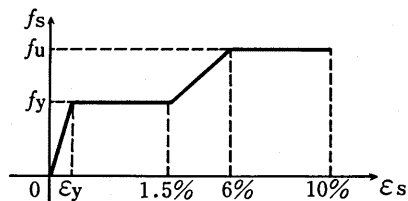


Fig. 4 Skelton curve of member



(a) concrete



(b) bar

Fig. 5 Stress-strain curves of materials

(3) Moment-Curvature Relationship and Displacement due to Flexure

Deflection of the RC member subjected to a bending moment was calculated on the basis of the moment-curvature relationship of a cross section. The following assumptions were made:

1. The plane section initially remains plane at any bending stage.
2. The section is divided into a number of elements, and in each element, strain and stress are assumed to be constant.
3. The position of the neutral axis of the cross section is determined so as to fulfill the equilibrium equation for axial force and bending moment.

(4) Additional Deflection due to the Elongation of Bars from Footing

Additional deflection (d_2) at the top point of the column due to the elongation of longitudinal bars from footing was calculated by means of the method proposed in a previous study [6], that is,

$$d_2 = h \cdot r = h \cdot l_0 \cdot \sigma_s / 2 \cdot x$$

(1)

where h = length of column.

r = rotation of bottom section of column.

ss = strain of longitudinal bar at the bottom section of column.

l_0 = the distance between the surface of the footing and the position of the bar strain of 0.

x = the distance between the neutral axis and the position of tension bars in the bottom section.

(5) Comparison of Measures and Predictions for Skelton Curves

The comparisons of measures and predictions for skelton curves were made in order to verify the validity of the model mentioned above.

In our experiment [8], the columns had a constant a/d ratio (4.0), while the longitudinal reinforcement ratio (0.950%--2.149%), the transverse reinforcement ratio (0.157%--0.357%) and axial compressive stress (0--40 kgf/cm²) varied. As for dy/dcy , dy and dcy = observed value and calculated value of displacement at member yielding, respectively; the mean value and the coefficient of variation were 0.99 and 6.0 %, respectively. As for du/dcu , du and dcu = observed value and calculated value of displacement at ultimate state, respectively; the mean value and coefficient of variation were 0.996 and 28%, respectively. Observed values of loads at member yielding and ultimate state were almost equal to calculated values. Furthermore, close agreements between observed and calculated values of displacement and load in the experiment regarding beams were obtained [2].

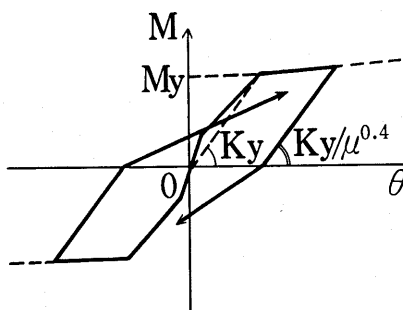
2.4 Hysteresis Loop of Member

Hysteresis loops of members were calculated as follows on the basis of experimental results of column [8] and beam [2],[9]:

A Takeda model [10], taking the occurrence of cracks into account, was applied for column members; unloading stiffness K' beyond member yielding was assumed to be $f^{-0.4} * K_y$ (f is ductility factor) (see Fig. 6(a)). And a modified Takeda model was applied for the beam members (see Fig. 6(b)).

2.5 Comparison of Measured and Calculated Force-Displacement Relationships of Rigid Frame Specimen

(a)column



(b)beam

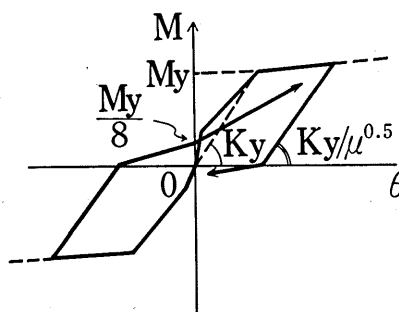


Fig. 6 Hysteresis loops for column and beam

A comparison between measured and calculated force-displacement relationships of two-story rigid frame specimen was made in order to verify the validity of the analysis method mentioned in 2.1--2.4.

Each rigid frame specimen had a size one quarter that of a standard rigid frame on the Tohoku Bullet Line (height 12 m). In the three specimens, the stiffness ratio of column to mid-height beams varied, (the ratios of the yield load of beams to the yield load of columns were 0.8, 0.2, 1.7 in specimens No. A, No. B, and No. C, respectively), while the dimensions of columns and upper beams and the longitudinal steel ratios were the same (see literature [11] for more detail). Figure 7 shows the measured and calculated envelope of P-d curves (P: horizontal force loaded at the top of the frame, d: horizontal displacement at the loading point). In this figure, calculated values taking only flexural deflection into account were also plotted for No. A, but this curve was considerably different from the observed curve. Figure 8 shows the comparison of measured and calculated force-displacement curves of specimen No. A, as one example, under alternating cyclic loading. For force-displacement curves of other specimens, close agreements between calculated and observed curves up to the ultimate state were obtained. Then, the force-displacement of the rigid frame was estimated on the basis of the assumptions in 2.1--2.4.

2.6 Static Elasto-Plastic Analysis of RC Viaducts, and the Relationship Between Results and Earthquake Damages

There were 105 two-story viaducts, the structural conditions of which were well documented, in Miyagi prefecture. But, while there were some viaducts having the same dimensions, there were 33 patterns of moment-rotation relationships of column or mid-height beam sections. Footing was assumed to be rigid.

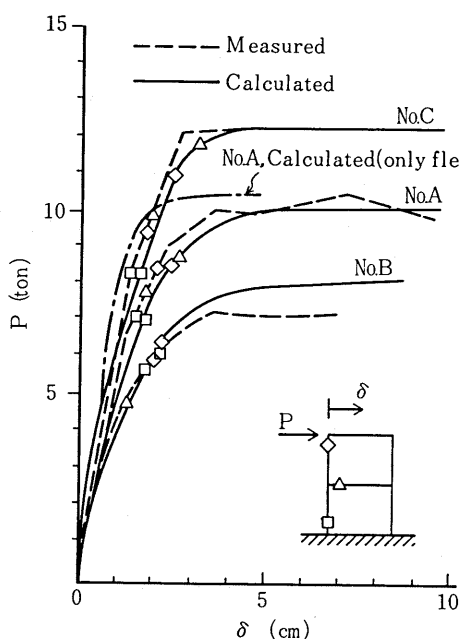


Fig. 7 Envelopes of P- δ curves

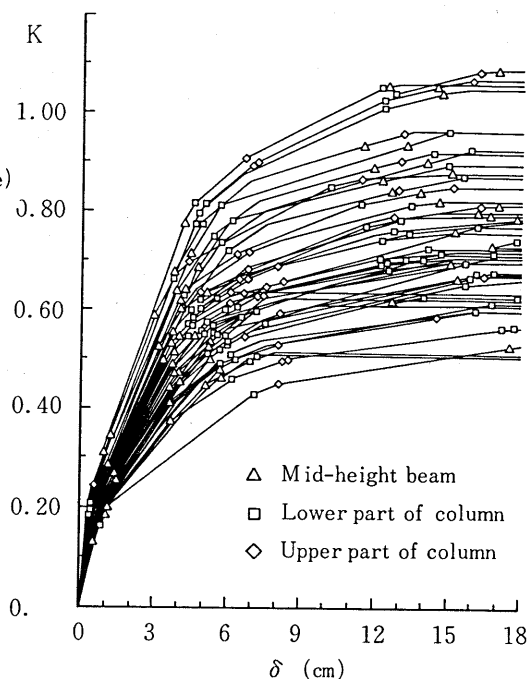


Fig. 9 Seismic coefficient-displacement of viaducts

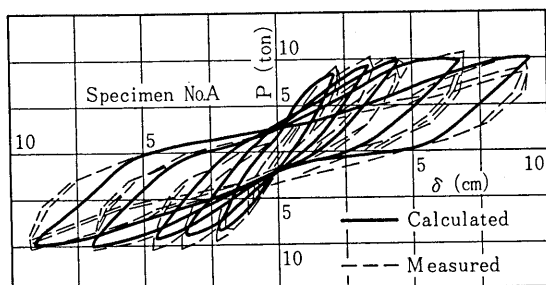


Fig. 8 P- δ curves of No. A under alternating cyclic loading

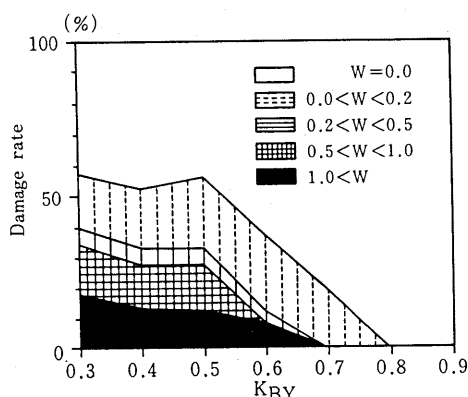


Fig. 10 Relationship between K_{by} and the ratio of earthquake damage

In static elasto-plastic analysis of viaducts, lateral force was applied to the column tip in viaducts. In this paper, the seismic coefficient K is defined as follows:

$$K = \frac{\text{(force applied to the tip of viaduct)}}{\text{(sum of weights of 1st story and 2nd story)}} \quad (2)$$

This seismic coefficient is defined as the base shear coefficient at the base of the lower part of the column. K_{bc} , K_{by} , K_{lc} and K_{ly} are defined as the seismic coefficients at the time of occurrence of diagonal cracks in the mid-height beam, time of yielding of the mid-height beam, yielding of the lower part of the column and yielding of the upper part of the column, respectively. A design equation presented by the CEB [12] was applied in calculating the occurrence of diagonal cracks.

Figure 9 shows the calculated results of the seismic coefficient-displacement at the top of the viaduct. In this figure, the positions of the symbols indicate the occurrences of flexural cracks, diagonal cracks, member yielding and the ultimate state in each member. Through this analysis, the following observations were made: there was considerable variation in the resistance of each actual structure, and yielding of the members in each structure occurred in the mid-height beams first, continuing into the lower part of the column and then the upper part of the column. The range of the ratio $K_{by}:K_{lc}$ was from 0.65 to 1.05. The mean value of the ratio was 0.9, and the ratio was less than 1.0 in more than 95 % of the viaducts. Furthermore, the ratio of $K_{bc}:K_{lc}$ was less than 0.55 in all viaducts (the mean value of the ratio was 0.4). Since K_{bc} and K_{by} were smaller than K_{lc} as mentioned above, the following phenomenon was understood to have occurred: yielding of mid-height beams preceded the yielding of columns.

Figure 10 shows the relationship between K_{by} and the degree of damage (the width of cracks was taken as the damage index). The presence of cracks was recognized in viaducts with a K_{by} of 0.8 or lower and some damage was recognized in about half the viaducts with a K_{by} of 0.5 or lower. With regard to a crack width of 0.2 mm or more, the percentage of the occurrence of cracks was about 40%. Only some structures with a K_{by} of 0.7 or lower suffered from cracks of a width of 1 mm or more, the percentage of the occurrence of cracks being about 15% or more for the structures with a K_{by} of 0.5 or lower.

The seismic coefficients K_d , (taking the ground type and the characteristics of response between the structure and ground in design of RC viaducts) were 0.2 or 0.25. The resistance of viaducts with a K_d of 0.25 was higher and the degree of damage was lower than in viaducts with a K_d of 0.2 (see Fig. 11).

Through the study of the relationship between the static elasto-plastic analysis of RC rigid frame and earthquake damage, the degree of earthquake damage of viaducts was related to the seismic coefficients at the time of yielding of mid-height beams (i.e., base shear coefficients).

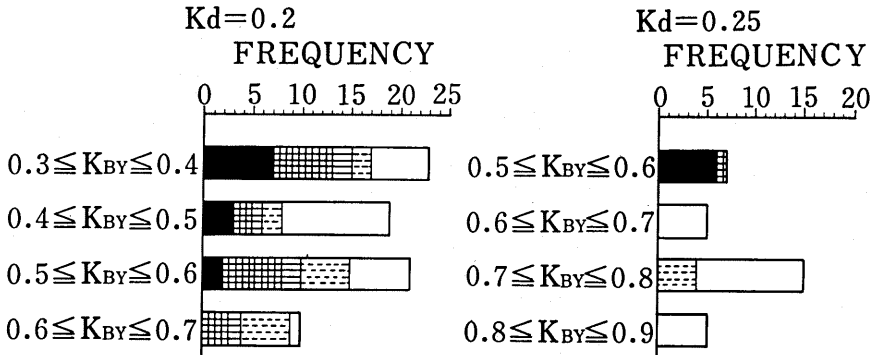


Fig. 11 Design seismic coefficient and damage ratio

3. DYNAMIC ANALYSIS OF VIADUCT AND EARTHQUAKE DAMAGE

A dynamic analysis of RC rigid frames with different ultimate seismic coefficients under actual earthquake waves was performed. The relationship between the responses of viaducts and earthquake damage was also investigated. And the amplification of earthquake waves on the surface of the ground was studied; using a transfer function, the relationship between amplified earthquake waves and earthquake damage was studied.

3.1 Method of Analysis

Three viaducts, having the same column dimensions, but different dimensions of mid-height beams and different ratios of reinforcing bars of mid-height beams were the subject of analysis (No. 1, No. 2 and No. 3). The bending moments at yielding of mid-height beams were different. Figure 12 shows the seismic coefficient-displacement of the top of these viaducts under loading from the top.

A vibration equation of the multi-mass system is written in general incremental form,

$$[M]\{\ddot{\Delta y}\} + [C]\{\dot{\Delta y}\} + [K(t)]\{\Delta y\} = -[M]\{1\}\ddot{y}_0 \quad (3)$$

where

$[M]$: mass matrix

$[C]$: damping matrix

$[K(t)]$: stiffness matrix

$\{\Delta y\}$: increment of horizontal displacement ($= y(t+\Delta t) - y(t)$)

$\{\ddot{y}_0\}$: acceleration of ground

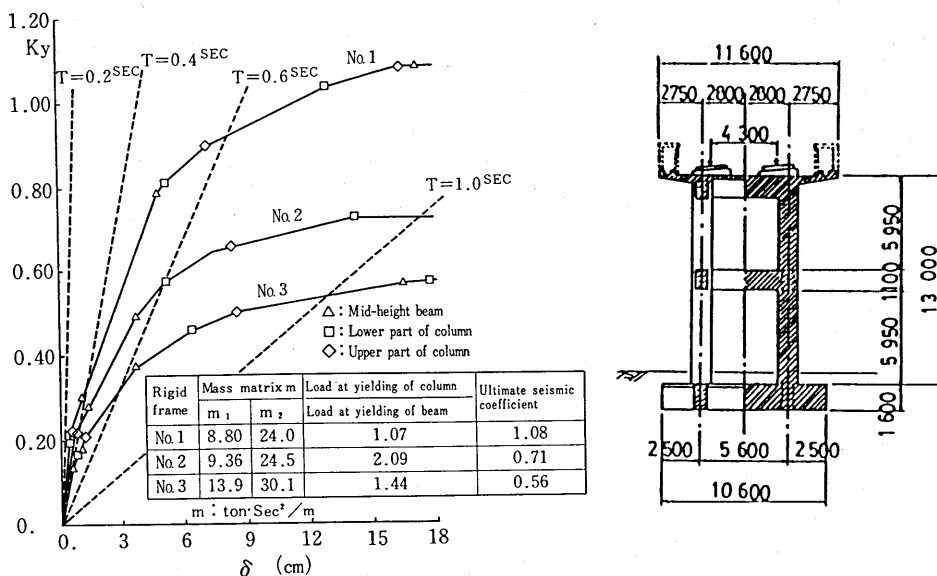


Fig. 12 Seismic coefficient-displacement of viaducts

Table 1 Characteristics of input waves

Earthquake	Record place	Max. accelerat-ion (gal)		Root sum square acceleration(gal)		Spectrum intensity(cm)	
		NS	EW	NS	EW	NS	EW
Miyagiken-oki	Sumitomoseimeji building (B2F)	250	240	44	41	107	96
	JNL (B1F)	432	232	70	47	164	98
	Tohoku Univ. (1F)	258	203	58	51	196	123
	Kaihoku bridge	L G 191	T R 273	24	36	25	69
EL-CENTRO		314	221	72	56	139	101
TAFT		174	154	33	34	60	67

In this analysis, the mass of a 2-story rigid frame was concentrated on each story, rotational inertia moments at node were ignored and horizontal displacements were taken into consideration. The β method proposed by Newmark ($\beta=1/4$) was used in numerical integration, time interval of calculation was $\Delta t=1/500$ sec. Tangential stiffness as seen in Fig. 6 was employed. Proportional damping type was employed as the damping matrix:

$$[C]=(2h/\omega) [K] \quad (4)$$

where

h : damping factor ($h=0.03$)

$$\omega : 2\pi/T_1$$

T_1 : natural frequency of first order of rigid frame

Some earthquake waves recorded in Sendai city during the Miyagiken-oki earthquake were used in this analysis. Maximum accelerations, root sum square acceleration, and spectrum intensity are shown in Table 1. The effect of ground type was not taken into consideration. Mass was assumed to be concentrated on the axis of the upper beam, the mid-height beam and the beams in the ground.

3.2 Results of Analysis

(1) Modal Analysis

Figure 13 shows maximum lateral displacements at each story of rigid frame No. 2. As the lateral displacement mode was estimated to be almost linear, the order of yielding in each member or lateral displacement mode was estimated by static analysis under loading at the top of viaducts.

(2) Dynamic Analysis

Dynamic analyses of rigid frames No. 1, No. 2 and No. 3 were made, and the ductility factors of the lower parts of columns and mid-height beams were investigated. In this analysis, the maximum acceleration of input waves varied from 200 gal to 700 gal. As a result, the maximum accelerations at which yield occurred in members varied according to input waves. The maximum accelerations at yielding of mid-height beams ranged from 430 gal to 700 gal for No. 1, and from 300 gal to 600 gal for No. 2 and No. 3. As acceleration in Miyagi prefecture during the Miyagiken-oki earthquake ranged from 200 gal to 500 gal, the mid-height beams in actual viaducts were apt to yield easily. Figure 14 shows one example of dynamic analysis of No. 2.

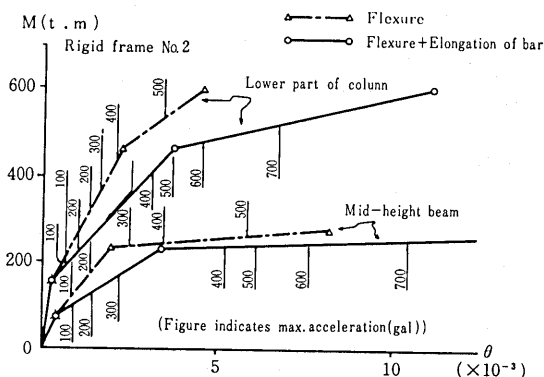
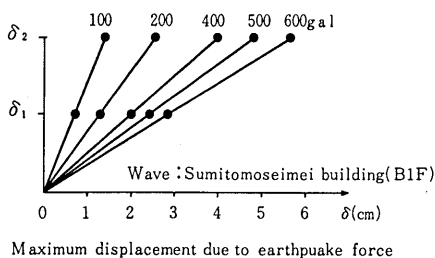


Fig. 13 Lateral displacement mode Fig. 14 Result of dynamic analysis of No.2

3.3 Ground and Damage

Stratiform ground above the base ground has specific vibration characteristics and has an influence in changing the characteristics of the input wave. In the following section, this influence is investigated by means of a transform function; its relationship with the damage is also studied.

(1) Response of Ground

Thickness, unit weight, velocity of shear wave and the damping factor in each layer must be known in order to evaluate the transfer function. Velocity of shear wave V_s was evaluated by the equation $V_s = 89.8 \cdot N^{0.341}$ (N:N-value) [13] regardless of the ground type. Unit weight of soil and the damping factor were assumed to be 1.7 tonf/m^3 , and 0.02, respectively. It is difficult to determine the base of ground in estimating the transfer functions. And responses may vary, according to the position of the input of the wave. But since N-values were not obtained beyond $N=50$, we investigated the amplification of the wave in this range and its relationship with earthquake damage. The velocity of a shear wave beyond $N=50$ was assumed to be 500 m/sec . As input wave into base of ground, the wave (EW: $\ddot{z}=241 \text{ gal}$) recorded in the Sumitomo-Building during the Miyagiken-oki earthquake, was employed, and half of \ddot{z} was inputted [14].

(2) Results of Analysis

Figure 15 shows the relationship between estimated acceleration and earthquake damage. Estimated acceleration ranged from 250 gal to 470 gal . Figure 16(a) shows the relationship between the ground type and the estimated acceleration. Estimated accelerations became greater gradually in ground types 1, 2, 3 and 4. The mean values of estimated accelerations were 275 gal , 320 gal , 406 gal and 424 gal in types 1, 2, 3, and 4, respectively. Figure 16(b) shows the relationship between the seismic coefficient at the time of yielding of mid-height beams (Kby), as mentioned in section 2, and the ground type. The mean

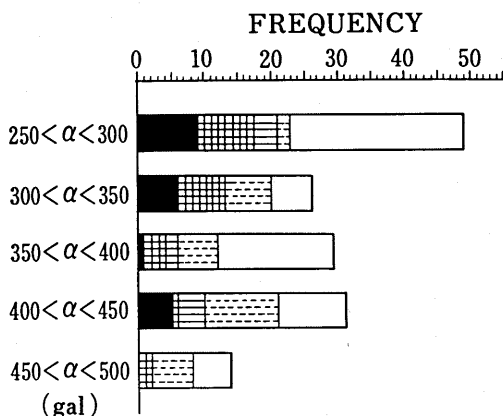


Fig. 15 Estimated acceleration and the rate of damage

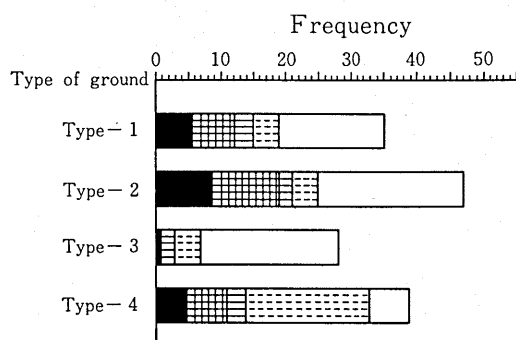


Fig. 17 Type of ground and the rate of damage

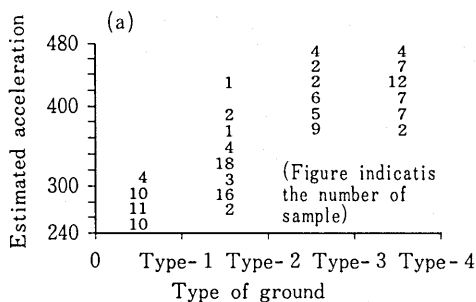
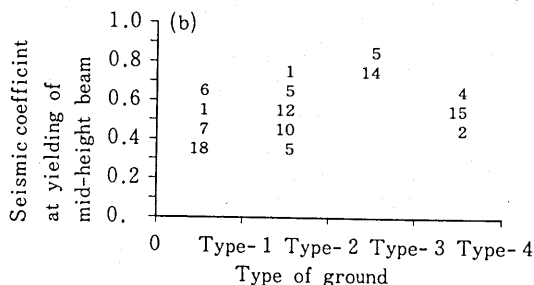


Fig. 16 Two dimensional arrange



values of K_{by} were 0.44, 0.51, 0.79 and 0.55 in types 1, 2, 3 and 4, respectively. The values may correspond to the degree of response of ground types in existing aseismic design. Figure 17 shows the relationship between the frequencies of damage and the ground type. One reason for the low rate of occurrence of damage in viaducts on the ground type 3 was that most of these viaducts were designed with a seismic coefficient of 0.25, and, therefore, these viaducts had the seismic coefficient at yielding of beams of 0.7 and more. Figure 18 shows the relationship between the ratio of K_{by} to estimated acceleration and the degree of damage. The smaller the ratio, the greater the damage.

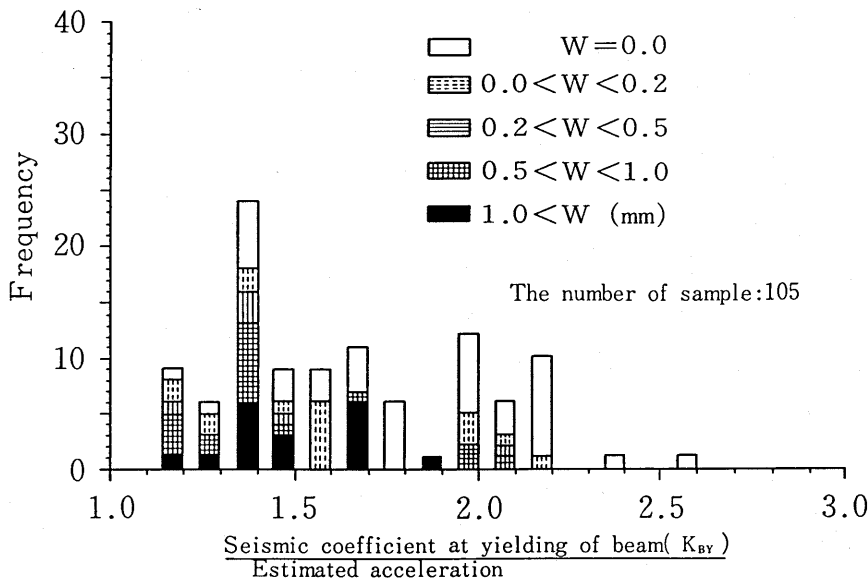


Fig. 18 The ratio of K_{by} to estimated acceleration and the rate of damage

4. STATISTICAL ANALYSIS OF DAMAGES OF RC VIADUCTS

4.1 Objection and Procedure

The aim of this section is to investigate the relationship between earthquake damage inflicted on RC viaducts and various factors such as structural conditions, ground conditions and so on, and to propose a model equation for damage evaluation. 149 viaducts constructed in Miyagi prefecture were surveyed through design books and/or field survey.

Explanatory variables were as follows:

- (A) Structural conditions: dimensions of members, ratio of bars, style of span, number of storeys, and so on.
- (B) Foundation conditions: style of foundation, type or style of pile, style and dimensions of footing, cover of soil and so on.
- (C) Ground conditions: ground type, the depth to ground base, the N-value, pattern of the N-value, pattern of the ground base, and so on. Figure 19 shows the classification of patterns of the N-value (from surface to ground

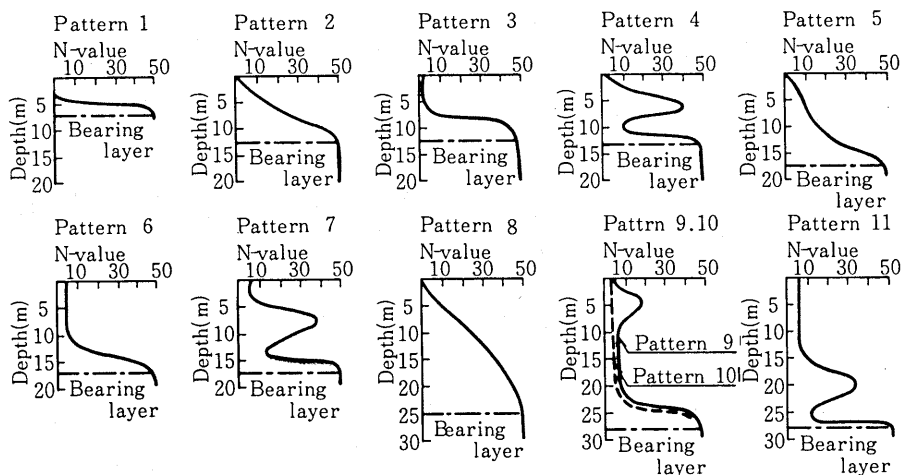
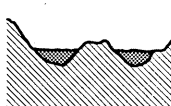
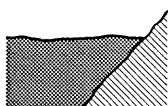


Fig. 19 Patterns of N-value

TypeA-1,2,3 TypeB-1,2,3 TypeC-1,2
Soft ground (10~20m) Soft ground(30~40m) Large change of bearing layer



TypeD-1,2,3
Stairway of bearing layer

TypeE-1,2,3
Fault

TypeF



TypeG
Mountain



Distance from the change of bearing layer
 { 1 : 0 ~0.5km
 { 2 : 0.5 ~1.0km
 { 3 : 1.0km~

Fig. 20 Patterns of bearing layer

Pattern	Pattern of crack
A	
B	
C	
No crack	

Fig. 21 Crack pattern

base with an N-value of 50). Figure 20 shows the classification of the patterns of ground base, taking the depth to the ground base or rock, inclination of the ground base and the distance of the structure from the sudden change point of inclination of the ground base.

(D) Earthquake force conditions: intensity scale, estimated acceleration, direction from epicenter, and so on.

(E) Situation at time of earthquake; age of mid-height beam, and so on.

Occurrence position, width, length, occurrence pattern (see Fig. 21) and so on, were surveyed for each crack.

4.2 Determination of Damage Index and Predictor Variables

(1) Determination of Criterion Variables (Damage Index)

For earthquake damages inflicted on viaducts, three factors -- maximum crack width, crack pattern and repair method of mid-height beams -- were integrated by means of the third method of quantification in order to make a damage index. The maximum crack width and the crack pattern expressed the character of the crack and the repair method was determined by examining the resistance of members.

Table 2 shows calculation results of 3 factors by means of the third method of quantification. The eigenvalue on the 1st axis was 0.94, and, therefore, three factors are represented on the 1st axis. The greater the degree of damage, the higher the category score on the 1st axis, and category scores for each factor were weighed satisfactorily. Therefore, sample scores on the 1st axis of the third method of quantification were used as a damage index.

(2) Determination of Predictor Variables

Coefficients of correlation between the damage index and explanatory variables were calculated; some explanatory variables which had a significant influence upon the crack occurrence were selected.

4.3 Evaluation of Damage

The first method of quantification was employed to calculate an equation for the evaluation of damage. The model equation of damage was as follows:

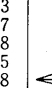


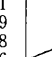
$$y_i = \bar{y} + \sum_{j=1}^R \sum_{k=1}^{m_j} Di(jk)w_{jk}^i \tag{5}$$

Table 2 Analysis results of damage by third method of quantification

Category		Axis	Axis-1	Axis-2	Axis-3
The number of data		Eigen value	0.936	0.829	0.495
Max. crack width	no crack	69	-0.376	0.194	0.138
	0.0<W≤0.5	49	0.123	-0.358	-0.408
	0.5<W≤1.0	10	0.128	-0.241	0.533
	1.0<W	21	0.405	0.360	0.005
Crack pattern	A	20	0.394	0.361	-0.051
	B	27	0.206	-0.323	0.428
	C	34	0.045	-0.267	-0.548
	no crack	68	-0.344	0.196	0.146
Repair method	no crack	86	-0.344	0.111	-0.074
	Injection of epoxy resin	48	0.254	-0.367	0.118
	reconstruction	15	0.371	0.390	-0.033

(note) W : crack width (mm)

Table 3 Result of factor analysis

ITEM	CATEGORY DATA				SCORE	RANGE
Integrated bearing layer pattern	1	A	49		-0.179	0.83
	2	B	33		0.273	
	3	C	7		0.341	
	4	D	8		-0.239	
	5	E	15		0.130	
	6	F	8		-0.489	
	7	G	4		0.306	
Integrated N-value pattern	1	1	79		0.003	0.02
	2	2	7		0.009	
	3	3	38		-0.009	
Ground type (1)	1	Type 1	35		0.017	0.22
	2	Type 2	46		-0.033	
	3	Type 3	4		0.191	
	4	Type 4	39		0.004	
Depth to the bearing layer (m)	1	0~10	51		0.138	0.73
	2	10~20	19		0.041	
	3	20~30	48		-0.089	
	4	30~40	6		-0.593	

CONSTANT=-0.02, R=0.724, R²=0.524

where

$D(jk)=1$: i responds to category k of factor j
 $D(jk)=0$: i does not respond to category k of factor j
 w_{jk} : normalized category weight corresponding to category k of factor j
 \bar{y} : mean value of objective variable

(1) Model Case

As mentioned above, one feature of the earthquake damage was as follows: viaducts with almost the same structural conditions on different ground types suffered from different levels of damage. Therefore, ground conditions were thought to be the main explanatory variable. The pattern of the ground base, the pattern of the N-value, ground type and the depth from the structure to ground base, which had higher correlations with damage were selected as explanatory variables (designated as case 1). In this case, as there were few data in two categories -- pattern of ground base and pattern of N-value -- these two factors were integrated, respectively (case 2). For the pattern of the ground base, the distance of the position of the structure from the sudden change of inclination of the ground base was omitted. And for the pattern of the N-value, only the shape of distribution of the N-value is taken into consideration.

(2) Results and Considerations

In case 1, the range in categories of the pattern of the ground base and the pattern of the N-value were wide, and, therefore, these two factors were thought to have a great influence on damage. The multiple correlation for case 2 was larger than that for case 1. And the ranges in category weight of the depth from the structure to the ground base or the prevailing period of ground were great. Table 3 shows the results of factor analysis for case 2 with the largest multiple correlation.

The influence of various predictor variables on earthquake damage were enumerated on the basis of the results of analysis.

Pattern of the ground base: in cases where the pattern of the ground base fell into categories A-1, B-3, C-1 and G, or into an integrated category of B and C, there was considerable damage in viaducts. And, therefore, in ground where the weak layer is deep (B) or the change of inclination of the ground base is sudden, interaction between the structure and the ground must be investigated in the future.

Ground type: category weights were negative for ground types 1 and 2, (i.e., there was little damage), and for ground types 3 and 4, the degree of damage was great. Viaducts constructed on alluvium suffered from considerably greater damage than those constructed on diluvium [15], and, therefore, more examinations of alluvium are required in the future.

Foundation type: damages inflicted on viaducts constructed on pile were great. These viaducts were constructed on ground type 2. Therefore, necessity of carefully selecting foundations must be stressed in the future.

Average of the N-value: the greater the average N-value, the lower the degree of damage. Thus, the N-value must be an important factor in aseismic design.

Prevailing period of ground: the longer the prevailing period of ground, the less the damage. As the prevailing period of viaducts was about 0.3 sec. [16],

the damages to viaducts were explained by the amplification of response.

5. ANALYSIS OF DAMAGES BY RELIABILITY THEORY

RC viaducts suffered damages according to district and ground conditions. It is important to take variance in the resistance of structures and applied earthquake forces into consideration, and to apply a reliability theory in order to understand the causes of earthquake damages. In the following section, a few points about earthquake damages are discussed by estimating the rates of damages.

5.1 Method of Estimating Rates of Damages

The reliability theory was used to calculate rates of damages. R and S are the probability variables, representing resistance of structure and applied earthquake force, respectively. Failure of structure is assumed to occur when the following inequality holds:

$$R \leq S \quad (6)$$

If R and S are independent, failure probability pf is represented by the following equation.

$$pf = \text{Prob}[R \leq S] = \int_0^{\infty} f_S(s) \int_0^s f_R(r) dr ds \quad (7)$$

where f_R and f_S are probability density functions of R and S , respectively.

If R and S represent the resistance of structures and applied earthquake force in a given district, pf is thought to be the rate of damage in the district. In this section, the rate of damage is calculated with respect to the above assumptions.

5.2 Variations of Resistance of Structure and Applied Earthquake Force

Seismic coefficients at yielding of mid-height beams by static analysis were employed, and the values calculated in section 3.3 were used for estimated acceleration.

(1) Variation of Resistance of Structure

Figure 22 shows the distribution of seismic coefficients at yielding of mid-height beams of 105 viaducts. The coefficient of variance of resistance of structures was about 20 %. The type of distribution was assumed to be normal.

(2) Variation of Applied Earthquake Force

If the applied earthquake force was represented by "ground acceleration" multiplied by "acceleration response magnification", and ground acceleration in a given area was almost equal, the variability of applied earthquake force was regarded as the variability of acceleration response magnification. Figure 23 shows the averages of 277 spectrum magnifications β for which the response spectrum was divided by the maximum input acceleration. The calculated values correspond to the response seismic coefficients for each natural period of a structure. As the yielding of mid-height beams occurred during increasing resistance, and initial natural frequency of viaducts was about 3 Hz, response

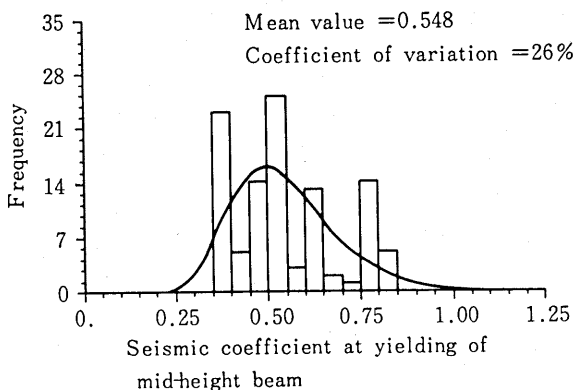


Fig. 22 Distribution of seismic coefficient at yielding of mid-height beams

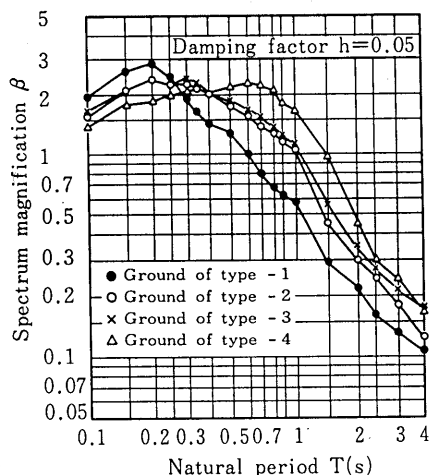


Fig. 23 Relationship between natural period and maximum acceleration response spectrum magnification

magnification for input maximum acceleration was estimated to be about 2. As the coefficient of variation of applied earthquake force was unknown, the value was assumed to be 40%, and distribution of the applied earthquake force was assumed to be log-normal.

5.3 Results and Considerations

Figure 24 shows the relationships between maximum ground acceleration G_{max} and the probabilities of occurrence of damage. The higher the average of R , the lower the probability of occurrence of damage. Judging from this analysis, K_{by} had an influence on the rate of damage occurrence.

As estimated by the overturning of tombstones, acceleration during the Miyagiken-oki earthquake ranged from 0.2g to 0.4g. Figure 25 shows the relationship between R (i.e., K_{by}) and the probability of damage occurrence for $G_{max} = 0.2g, 0.3g$, and $0.4g$. The input acceleration had a major influence on the occurrence of damage.

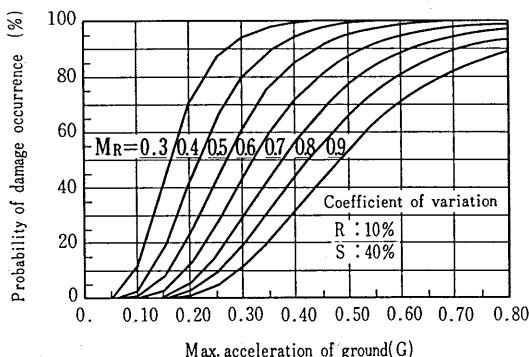


Fig. 24 Relationship between maximum ground acceleration G_{max} and the probability of occurrence of damage

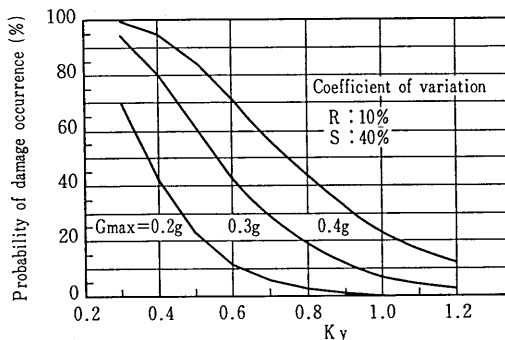


Fig. 25 Relationship between K_{by} and the probability of damage occurrence

Table 4 Ground type and the rate of damage (comparisons between measured and calculated values)

Type of ground		Type1	Type2	Type3	Type4
Seismic coefficient of mid-height beam	Mean m_R	0.443	0.512	0.793	0.548
	C.O.V (%)	20.8	17.8	1.4	9.3
Estimated acc. G_{max}	Mean (gal)	257	320	347	406
	C.O.V (%)	3.0	13.3	7.0	5.9
Damage rate (%)	Calculated	55	65	31	79
	Measured	54	53	25	85
Signified damage rate (%)		30	30	30	30
Seismic coefficient m'_R m'_R/m_R		0.61	0.74	0.79	0.93
		1.4	1.5	1.0	1.7

Next, we will consider 4 groups of structures for four ground types. Table 4 shows comparisons between observed and calculated values of rates of damage of structures for each ground type. Calculated values agreed approximately with observed values. Input data for the calculations were given in Table 4.

A rational design method would take into account the fact that the rate of damage of structures on different ground types would be almost the same against the same earthquake. On the basis of this consideration, if the rates of damage of structures on different ground types were equalized (ex 30 %), resistance of beams must be increased up to 1.4 --1.7 times that of the existing resistance as shown in Table 4.

Maximum input ground accelerations of an earthquake wave into structures varied according to ground type (see Table 4). If acceleration on ground type 1 is assumed to be 1, accelerations on ground types 2, 3, and 4 become 1.25, 1.35 and 1.58, respectively. These values would be significant for taking the different characteristics of vibration according to ground types into account with respect to aseismic design.

6. CONCLUSIONS

The causes of the concentration of damage in mid-height beams and the causes of different degrees of damage, according to district or ground type were investigated analytically and statistically. The following results were obtained:

(1) Judging from static analysis of RC viaducts, the yielding of mid-height beams occurs before the yielding of columns, that is, the order of yielding of members was, first, mid-height beams, followed by the lower part of columns and then the upper part of columns.

(2) Seismic coefficient K_{by} (base shear coefficient) at yielding of mid-height beams had an influence on the degree of damage in mid-height beams. For example, about half of the viaducts with a K_{by} of 0.5 or less suffered from some damage, about 40% of viaducts suffered crack damage of a width of 0.2 mm or more, and about 15% of viaducts suffered crack damage of width of 1 mm or more.

(3) Through dynamic analysis, estimated acceleration of 200 gal to 500 gal was found to be sufficient to cause yielding of mid-height beams.

(4) Acceleration estimated by means of a transfer function within an N-value of 50 or less ranged from 250 gal to 470 gal. The reason why viaducts constructed on ground type 3 suffered little damage is that these viaducts were designed with seismic coefficients of 0.25, and seismic coefficients at yielding of mid-height beams were rather high.

(5) Statistical analysis of damage was done. Viaducts where the weak layer was deep, the change of inclination of the base layer was sudden, the average N-value was low or the depth to the bearing layer was deep, suffered severe damage.

(6) Analysis of the damage rate on the basis of reliability theory was also done.

REFERENCES

- [1] JNR Sendai Shinkansen Construction Bureau : Senkanko '78 Miyagiken-oki Earthquake Special Issue, December 1979.
- [2] Y. Ozaka, M. Suzuki, H. Ishida and K. Kato : Study on Shear Failure and Repair Method of Reinforced Concrete Beam, Proc. of JSCE, No.360, pp.119-128, August, 1985.
- [3] M.F. Giberson : Two Nonlinear Beams with Definition of Ductility, Proc. of ASCE, Vol. 95, No. ST2, pp.137-157, Feb., 1969.
- [4] T. Shiga, A. Shibata, J. Shibuya and J. Takahashi : Observations of Strong Earthquake Motions and Nonlinear Response Analyses of the Building of Architectural and Civil Engineering Department, Tohoku University, Transactions of the AIJ, No. 301, pp.119-130, March, 1981
- [5] H. Shiohara, S. Otani and H. Aoyama : Effect of Member Modelling on Earthquake Response of RC Structure, Proc. of JCI 5th Conference, pp.217-220, 1983.
- [6] Y. Ozaka, T. Yanagida, M. Ota and J. Kadera : Dynamical Analysis of Reinforced Concrete Pier in Elasto-Plastic Range and its Application to Practical Design, Proc. of JSCE, No. 297, pp.71-85, May, 1980.
- [7] ACI : Building Code Requirements for Reinforced Concrete (ACI 318-83)
- [8] Y. Ozaka and M. Suzuki : Behaviours of Reinforced Concrete Columns under Static Alternating Cyclic Loads, Concrete Library of JSCE, No.10, pp.45-62, December 1987
- [9] H. Kikuchi, T. Sato and M. Suzuki : Modelling of the Force-Displacement Curves of RC Beams under Alternating Load, Proc. of JSCE 38 th Annual Meeting, V-183, pp.363-364, Sept., 1983.
- [10] T. Takeda, M.A. Sozen and N.N. Nielsen : Reinforced Concrete Response to Simulated Earthquake, Proc. of ASCE, Vol. 96, ST.12.
- [11] T. Ishibashi and S. Yoshino : A Study on the Earthquake-Proof of RC Rigid Frame, Proc. of JCI 5th Conference, pp.221-224, 1983
- [12] CEB : CEB-FIP Model Code for Concrete Structures, Bulletin d'information N.124/125E, Avr., 1978.
- [13] K. Toki : Aseismic Analysis of Structure, pp 74, GIHODO
- [14] A. Shibata : New Aseismic Structural Analysis, pp.231-238, MORIKITA
- [15] T. Siga : Study on the Prediction and Mitigation of Seismic Hazard to Urban Systems, Ministry of Education Scientific Research Fund Natural Disaster Special Study No.A-58-1, pp.127-137, March, 1984
- [16] K. Kato, H. Ishida and K. Matsuoka : Failure Mechanism and Repair Method of Mid-height Beams of RC 2-Story Viaducts, Proc. of JSCE 35th Annual Meeting , V-8, pp.15-16, Sep., 1980
- [17] JRA : Specification for Highway Bridge, V. Aseismic Design , pp.115, 1980